Electronic Supplementary Material (ESI) for Nanoscale.

Electronic Supplementary Information for

Polarity-tunable spin transport in all-oxide multiferroic tunnel junctions

Rohit Soni,[a] Adrian Petraru,[a] Harikrishnan S. Nair,[b] Ondrej Vavra,[a] Martin Ziegler,[a] Seong Keun Kim,[c] Doo Seok Jeong*[c] and Hermann Kohlstedt*[a]*

[a]Nanoelektronik, Technische Fakultät, Christian-Albrechts-Universität zu Kiel, Kiel 24143, Germany.

[b]Highly Correlated Matter Research Group, Physics Department, University of Johannesburg P. O. Box 524, Auckland Park 2006, South Africa.

[c]Centre for electronic Materials, Korea Institute of Science and Technology, Hwarangno 14-gil 5, Seongbuk-gu, Seoul 02792, Republic of Korea.

*E-mail: dsjeong@kist.re.kr, soro@tf.uni-kiel.de, and hko@tf.uni-kiel.de

1. Structural analysis of symmetric MFTJ

Fig. S1a shows the x-ray diffraction (XRD) patterns of an as-grown LSMO/PZT/LSMO heterostructure on a (001) SrTiO3 (STO) substrate. The 2q-w scan exhibits only (00l) peaks of the LSMO and PZT films, showing that these films are (001)-oriented, i.e. identical to the substrate. In order to check the in-plane orientation of the films, f scans were performed for the (101) diffraction peaks of the films and STO substrate, as shown in Fig. S1b. The f scans confirm the cube-on-cube epitaxial growth nature of the LSMO and PZT films. The rocking curve measurements (w scan) on the (002) reflection of the STO substrate (not shown) and PZT layer (Fig. S1c) identify a full width at half maximum (FWHM) of approximately 0.031° and 0.045°, respectively. The four-fold symmetric (101) peaks and FWHM values suggest the high-quality of the heterostructure.

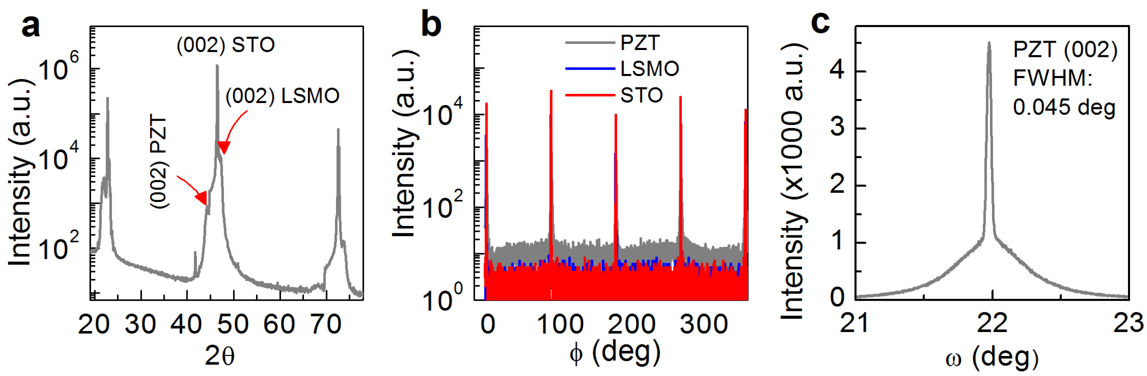

Figure S1. (a) XRD θ-2θ scan of a LSMO/PZT/LSMO heterostructure grown on a (001)-oriented STO substrate. A peak from the (002) plane of each layer is indicated. (b) ϕ scan of (101) reflection of the PZT/LSMO and STO underneath. (c) ω scan of (002) reflection of the PZT layer.

2. TER behaviour of MFTJ

Another order parameter (ferroelectric polarization) surely determines the tunneling current in ferroelectric tunnel junctions (FTJs), as seen in various FTJs.[1-4] Assuring genuine MFTJs therefore requires the presence of TER (at zero magnetic-field) as well as TMR. In this light, square voltage pulses (pulse width: 100ms) of different amplitudes (0.5 – 2.5 V) were applied to the FMTJ in an attempt to write the ferroelectric state: polarization up ($P^{\uparrow}$) and down ($P^{\downarrow}$) states. A pair of write voltage (V_w) pulses of different polarities (but with the same amplitude) was used to flip the spontaneous polarization, and a read-out voltage (V_r) followed each write voltage pulse to read the resistance, as illustrated in the inset of Fig. S2a. Consequently, a TER ratio given each pair of write voltage pulses was acquired, which is defined by ($R^{\downarrow}$-$R^{\uparrow}$)/$R^{\uparrow}$, where $R^{\downarrow}$ and $R^{\uparrow}$denote the resistance (V_r = 5 mV) written by a positive and negative voltage pulse, respectively. A stepwise increase in write voltage pulse amplitude was continued up to 2.5 V to achieve different intermediate ferroelectric states–mediated by ferroelectric domains–between complete $P^{\uparrow}$and $P^{\downarrow}$ states. As seen in the measurement results at 80 K in Fig. S2a, two resistance states $R^{\downarrow}$ and $R^{\uparrow}$evolve with write voltage that exceeds a *threshold* (ca. 1 V). The difference in resistance between the two states increases with write voltage; therefore, the TER ratio rises, exceeding 100% at 2 V (Fig. S2b). Such a gradual change in TER upon write voltage has been seen in similar FTJs.[5, 6]

The two states programmed by V_w = ±2 V ($R^{\downarrow}$ and $R^{\uparrow}$) were identified in their *I-V* behaviours; they are clearly distinguishable in the entire voltage range, as plotted in Fig. S2c. Notably, both states represent nonlinear *I-V* behaviour so that the TER ratio relies on read-out voltage. In addition, the two states are stable at 80 K showing negligible changes in resistance up to 3600 seconds of waiting time (the upper panel of Fig. S2d). The switching endurance of the MFTJ was also examined for $V_w = \pm 2$ V, and the results are shown in the lower panel of Fig. S2d. The TER effect was reproducible with an average 100% TER ratio for 50 switching cycles at 80 K in spite of fluctuation to some extent.

Inferring *a priori* that the observed TER effect is attributed to ferroelectric switching, i.e. ferroelectric-driven TER (FE-TER), saturating$R^{\downarrow}$ and $R^{\uparrow}$ implies complete $P^{\downarrow}$ and $P^{\uparrow}$ states, respectively. In this regard, the gradual evolution of $R^{\downarrow}$ and $R^{\uparrow}$ in Fig. S2a likely indicates the intervention of ferroelectric domains in the TER in the given range of write voltage. Complete downward switching ($P^{\uparrow} \rightarrow P^{\downarrow}$) appears to be achieved at a voltage larger than 2.5 V so that it may remain out of reach in the given write voltage range (0.5 V – 2.5 V). However, the decline in the rate of TER ratio increase with write voltage (>2 V) alludes to complete downward switching at slightly above 2.5 V. By contrast, complete upward switching ($P^{\downarrow} \rightarrow P^{\uparrow}$) is achieved in the voltage range with regard to the saturation of $R^{\uparrow}$at approximately -2.5 V. Recalling the coercive voltage obtained from the PFM measurements at room temperature (~0.18 V), a large disparity between the PFM and TER measurement results lies in coercive voltage. Invoking the thermal activation of ferroelectric switching[7], the disparity perhaps arises from different measurement temperatures: 80 K and room temperature for the TER and PFM cases, respectively. Additionally, the voltage application method can substantially alter the ferroelectric switching kinetics, leading to the difference in coercive voltage. Note that it still remains challenging to identify the quantitative correlation between TER and ferroelectric switching in an ultrathin ferroelectric film in a fully structured tunnel junction. Later, we will provide evidence for the FE-TER effect in our MFTJ by differentiating it from the redox-based resistance-switching effect that often misleads.

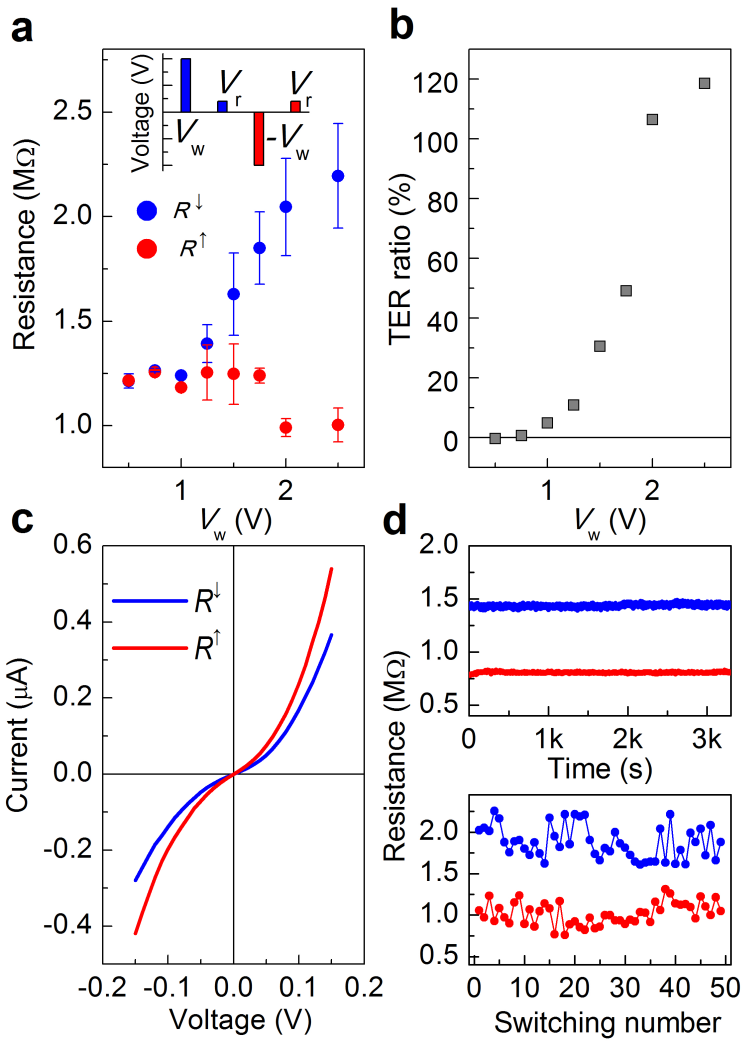

Figure S2. (a) Resistance-change of the MFTJ upon the application of a write voltage pulse of 10 ms duration. A set of voltage pulses–positive write (V_w), read-out (V_r: 5 mV), negative write (-V_w), and the same read-out (V_r: 5 mV) voltage pulses–was applied to the TE. The amplitude of the write voltage pulse ($|V_w|$) rose from 0.5 to 2.5 V. (b) Evaluated TER ratio after each pair of write pulses. (c) Quasi-static *I-V* behaviour for two distinctive polarization states ($P^{\downarrow}$ and $P^{\uparrow}$) that were achieved by poling the tunnel barrier by applying a V_w = 2 V and -2 V, respectively. (d) Upper panel: retention of the two states (at V_r = 5 mV). Lower panel: reproducibility of the reversible

3. Effect of ferroelectric-writing voltage on TMR at 80 K

The TMR ratio loops that correspond to the resistance vs. magnetic-field loops are plotted in **Figure S3**.

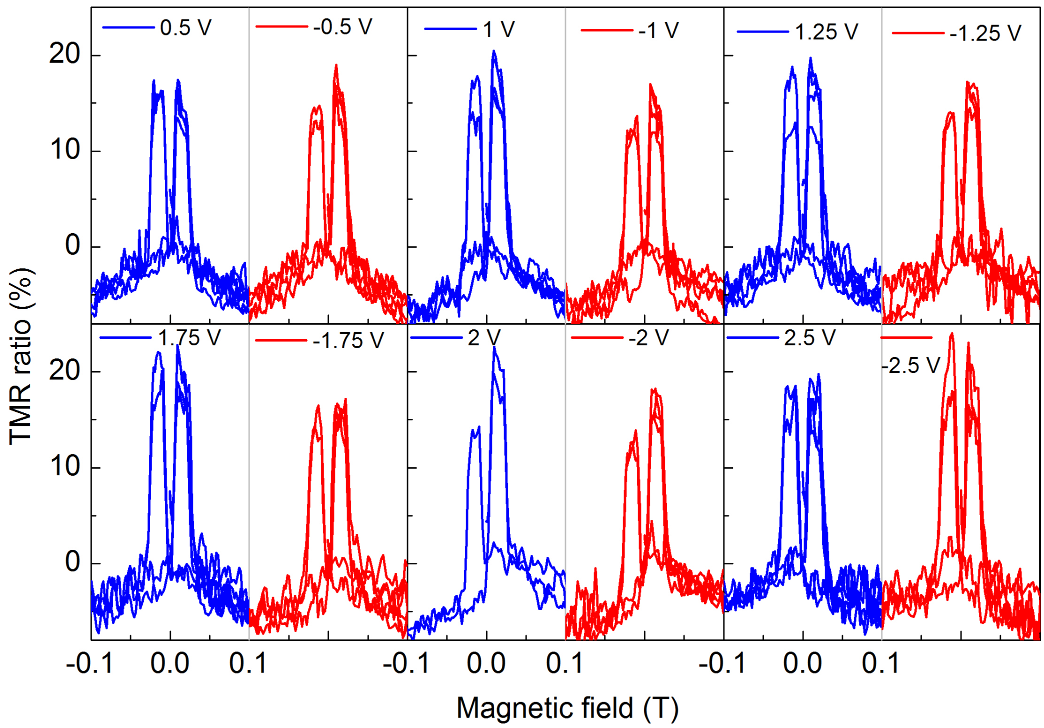

Figure S3. TMR ratio after each writing voltage was evaluated from the corresponding resistance versus magnetic field hysteretic loop in Fig. 2a.

4. Various resistance-states in current-voltage plane

Four different resistance states ($R_P^{\downarrow}$, $R_{AP}^{\downarrow}$, $R_P^{\uparrow}$, and $R_{AP}^{\uparrow}$) have different current-voltage characteristics as shown in **Figure S4**.

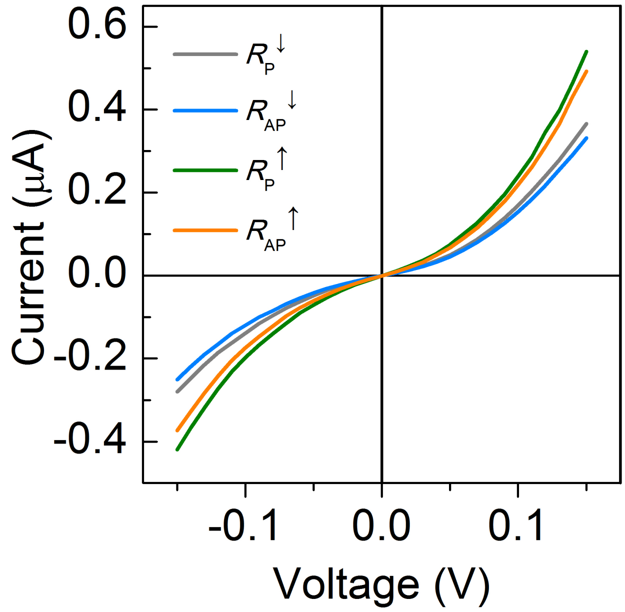

Figure S4. I-V behaviour in four distinctive states.

References

1. E. Y. Tsymbal and H. Kohlstedt, *Science*, 2006, **313**, 181.
2. R. Soni, A. Petraru, P. Meuffels, O. Vavra, M. Ziegler, S. K. Kim, D. S. Jeong, N. A. Pertsev and H. Kohlstedt, *Nat Commun*, 2014, **5**, 5414.
3. A. Gruverman, D. Wu, H. Lu, Y. Wang, H. W. Jang, C. M. Folkman, M. Y. Zhuravlev, D. Felker, M. Rzchowski, C. B. Eom and E. Y. Tsymbal, *Nano Lett.*, 2009, **9**, 3539.
4. E. Y. Tsymbal, A. Gruverman, V. Garcia, M. Bibes and A. Barthélémy, *MRS Bull.*, 2012, **37**, 138-143.
5. A. Petraru, R. Soni and H. Kohlstedt, *Phys. Status Solidi Rapid Res. Lett.*, 2012, **6**, 138-140.

6. P. Maksymovych, S. Jesse, P. Yu, R. Ramesh, A. P. Baddorf and S. V. Kalinin, *Science*, 2009, **324**, 1421.

7. Y. W. Yin, J. D. Burton, Y. M. Kim, A. Y. Borisevich, S. J. Pennycook, S. M. Yang, T. W. Noh, A. Gruverman, X. G. Li, E. Y. Tsymbal and Q. Li, *Nat Mater*, 2013, **12**, 397-402.